Experimental Evaluation of Catalysts for Monopropellant Hydrazine Propulsion

H. GREER,* S. M. KING,† P. C. MARX,† AND D. TAYLOR‡
The Aerospace Corporation, El Segundo, Calif.

Many monopropellant propulsion systems use a catalyst to decompose hydrazine. Problems of catalyst attrition have given rise to various special processes intended to improve catalyst durability. Precalcined and rounded catalysts were evaluated by measurements of mechanical properties and motor firing characteristics. The results were compared to those obtained with the original catalyst. For the conditions tested, no significant differences in performance or in catalyst activity were observed, and only the precalcining process resulted in a reduction in catalyst loss and breakup. Laboratory measurements of porosity and of thermal expansion coefficient indicate that this improvement is probably due to less catalyst shrinkage and to a more open pore structure.

Introduction

A CATALYST for the decomposition of hydrazine (N_2H_4) should have high-specific activity, high-thermal conductivity and low-thermal expansion, high-thermal stability and resistance to thermal shock, and good mechanical strength. A composite catalyst is used to satisfy these criteria. This catalyst, composed of an active metal deposited on the carrier of porous alumina, is prepared from components of controlled purity using special techniques[1] for an optimum combination of specific surface area, high mechanical strength and resistance to thermal shock.

Early granular catalyst,§ designated 405-ABG,¶ used a carrier that was slightly attrited by tumbling.[2] As the number of applications increased, problems arose concerning the effects of vehicle vibrations and extended firings on the structural integrity of the catalyst. The ABSG (spheroidal granules) processes, which remove irregular shaped particles with weak and fissured projections by either air or water attrition, were developed to improve the capability of the catalyst to withstand mechanical stresses. Figure 1 shows the, a) untreated 25–30 mesh carrier and its appearance after, b) water- or, c) air-attriting to approximately 50% of the original weight.

Since the catalyst pore surface area was observed[3] to decrease with use, one user specified calcining the alumina support at 900°C for 1 hr as a means of stabilizing operation and of improving performance. The purpose of this study is to measure and evaluate the characteristics of catalysts treated by these processes and to determine the mechanisms of catalyst breakup and loss.

Mechanical Strength

Catalyst breakup and loss through mechanical attrition was measured by gas-blast, vibration, crush, and cyclic load tests. The amount of attrition produced by the reaction chamber loading and screening procedures was examined first. The chambers were vibration-packed using a 52.5-g piston (load of 0.59 lb/in.^{2}) to settle the material to a constant depth, and no significant attrition was observed. The material in the beds was weighed before and after each test to determine loss. Breakup was determined by sieving the material remaining after testing to the following mesh size fractions >30, 30–40, 40–60, and <60. Three tests were normally made and averaged.

Table 1 presents results of gas-blast and vibration tests. For the gas-blast tests, a Lucite chamber with the same dimensions as the metal reaction chamber, Table 2, was used. A 0.40-in. bed length was produced by a 1.2-in. spacer with a 60-mesh catalyst support screen. Bed void spaces of 0, 5, and 10% (excluding intergranular voids) were obtained by vibration-packing the catalyst using the 52.5-g position piston and depth-gaging the compaction distance. Each bed was subjected to 1720 gas pulses (0.5 sec On, 1 sec Off) in an upward direction at chamber pressure of approximately 125 psi. The results for carriers indicate some breakup for the 10% void space tests, but no detectable loss from the chamber. The water-attrited carrier appears to be best. Although no appreciable attrition was indicated for the 0 and 5% void

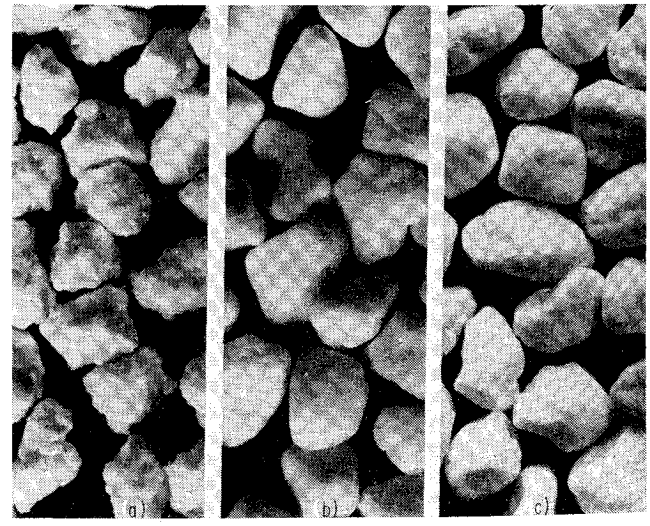

Fig. 1 Carrier samples: a) as-received, b) water-attrited, and c) air-attrited carrier.

Received March 9, 1970; revision received July 20, 1970.

* Member of the Technical Staff, Applied Mechanics Division. Associate Fellow AIAA.

† Member of the Technical Staff, Aerodynamics and Propulsion Research Laboratory.

‡ Member of the Administrative Staff, Aerodynamics and Propulsion Research Laboratory.

§ Shell Development Co., Emeryville, Calif.

¶ ABG denotes alumina (Reynolds Metals Co., Richmond, Va.), granular.

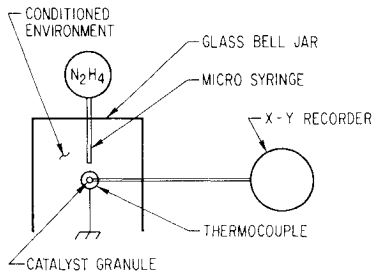

Fig. 2 Schematic of laboratory thermocouple activity apparatus.

space catalyst tests, breakup and loss occurred at 10% voids.

The lower part of Table 1 shows that vibration is not a source of severe attrition. For these tests, the Lucite chamber was vibration-packed and positioned on an electromagnetic vibration exciter so that the direction of generated forces was at right angles to the length of the catalyst bed. The samples were exposed to vibration for 10 min at a level equivalent 1.0 g^2/Hz between 400 and 1000 Hz, using 11-cycle increments of 55-sec duration each.

Crushing strength determinations were made by loading samples of the 25–30 mesh carriers and catalysts to a depth of 0.23 in. in a 0.50-in. die, vibration-packing them, and then compressing them 0.02 in. and 0.04 in. The results are given in Table 3. The ABSG air-attrited and calcined carrier displayed a marked decrease in load-bearing capability compared with the uncalcined, air- and water-attrited carriers. Again the water-attrited carrier displayed more favorable load-bearing characteristics than the air-attrited carrier, and both attrited carriers had greater load-bearing capabilities than the untreated carrier. Catalysts produced from air-attrited, and air-attrited-calcined (900°C for 1 hr) carriers displayed similar characteristics.

For the repeated-load tests, the carrier was loaded into the 0.50-in. die, as previously described, and compressed 0.02 in. The compression load was observed and set on the tester. Three samples were cycled to the same load 5, 20, and 100 times, and final deflection was obtained. Fragmentation increased as cycling increased (Table 4). A correlation was noted between fragmentation and final degree of compression, whether single-stroke or repeated-loading. The water-attrited carrier appears to have superior load-bearing capability but does not show any marked superiority in fragmentation characteristics.

Thermal Shock and Thermal Expansion

The catalyst was heated in an open quartz tube to 1000°C and quenched with a jet of water (sauna treatment), decreasing the temperature to 100°C in approximately 0.5 sec. Since there was no evidence of fracture during six heat-and-quench cycles with samples of ten pellets and of ten 14- to 18-mesh granules, excellent thermal shock resistance was indicated.

Granular and pellet catalyst expansion and contraction measurements were made using a dilatometer. Each run in Table 5 represents a 6-hr. heating and cooling cycle from 25°C to 1080°C and back to 25°C. In the first run, using a single $\frac{1}{8}$-in. pellet, a net shrinkage of 1.2% was recorded at 1000°C. At the completion of the cycle, the net shrinkage had increased to 4.8%. The next three runs comprised a series of three cycles using 25–30 mesh ABSG air-attrited catalyst packed in a quartz tube between two quartz rod-plungers. The granule train tended to expand as it was heated to 1000°C, and the net expansion at 1000°C increased with each cycle. In the third cycle, this expansion approximated the linear expansion of fully dehydrated crystalline α-alumina (an expansion of 0.9% from 25°C to 1000°C). However, a full cycle of heating and cooling produced a net shrinkage even after three cycles. This result is attributed to the conversion of hydrated alumina to the α form, a process which is accompanied by shrinkage and is slow even at 1080°C.

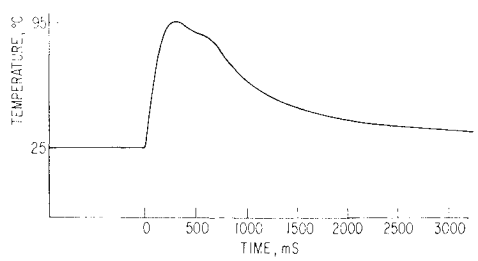

Fig. 3 Hydrazine—catalyst temperature transient.

Table 1 Gas blast attrition[a] and vibration[b] test results for three levels of bed void space (0/5%/10%) under each column

ABSG carrier used	Weight, g	Average wt %, U.S. sieve size[b,c] 30–40	40–60	<60
Gas blast,[a] carrier only				
Air-attrited	1.46/1.41/1.35	2.3/2.4/4.9	S/S/S	S^2/S^2/S^2
Water-attrited	1.47/1.43/1.36	2.1/0.7/0.7	S/S/S	S^2/S^2/S^2
Air-attrited (cal. 900°C, 1 hr)	1.36/1.32/1.25	4.1/4.2/7.3	S/S/0.8	S^2/S/S
Gas blast,[a] catalyst				
Air-attrited	2.09/1.98/1.88	1.4/1.8/7.8[d]	S/S/2.7	S/S^2/0.7
Air-attrited (cal. 900°C, 1 hr)	2.05/1.95/1.85	1.7/1.5/3.8[e]	S/0.5/0.9	S/S/S
Vibration,[b] carrier only				
Air-attrited	1.38/1.33/1.35	3.0/2.7/2.1	S/S/S	S/S/S
Water-attrited	1.38/1.34/1.26	1.2/0.9/1.0	S/S/S	S/S/S
Vibration,[b] catalyst				
Air-attrited	2.09/1.98/1.88	0.9/0.7/1.3	S/S/S	S^2/S^2/S^2

[a] 0.40-in. bed depth, 1700 pulses in an upward direction @ 125 psi.
[b] 0.40-in. bed depth, 400–1000 cps @ 1.0 g^2/cps.
[c] Balance (not shown) is >30-mesh material remaining (e.g., 97.7% for first sample, 0 void) or loss; see footnotes d, e.
[d] S = small, <0.1%; S^2 = small, <0.1%, two samples taken.
[e] Loss = 4.7% in 10% void sample.

Laboratory Activity Tests

An index of catalyst activity was obtained in the laboratory by measuring the rate and magnitude of the temperature rise occurring when a measured droplet of N_2H_4 contacts a catalyst pellet or granule with a chromel-alumel thermocouple embedded in the catalyst surface, Fig. 2. Initial catalyst temperature was varied from −20°C to +75°C by directing a stream of thermally conditioned nitrogen over the catalyst surface until the desired temperature was reached.

Table 2 Reactor design characteristics

Chamber diameter, D_c, in.	0.51
Nozzle throat diameter, D_n, in.	0.088
Nozzle exit diameter, D_e, in.	0.62
Catalyst bed length, L_c, in.	0.56
Total chamber length, in.	2.10
Total chamber volume, cm^3	7
Injector volume, cm^3	0.25
Reservoir pressure, psia	315
Steady-state design downstream chamber pressure, P_c, psi	235
Steady-state downstream gas temperature, T_c, °F	1700
Steady-state design flow rate, ml/sec	5
Steady-state design bed loading G, lb/sec-$in.^2$	0.054
Nominal initial weight of 25–30 mesh catalyst, g	3

Table 3 Crush tests[a]

Carrier used	0.02-in. Compression						0.04-in. Compression				
	Wt, g	$\bar{P}$, psi	Avg. wt %, U.S. sieve size >30	>40	>60	<60	$\bar{P}$, psi	Avg. wt %, U.S. sieve size >30	>40	>60	<60
Carrier only											
ABSG, air-attrited	0.87	1722	78.7	11.1	4.6	5.7	4213	57.2	16.3	10.0	16.6
ABSG, air-attrited (13.3% H_2O adsorbed)	0.94	1752	85.0	7.8	3.2	4.0					
ABSG, air-attrited (14.7% H_2O adsorbed)	0.95	1798	85.4	6.6	3.3	4.7	4065	60.9	14.5	8.7	16.0
ABSG, air-attrited (18 hr @ 100°C-vac.)	0.84	2150	85.6	7.4	3.2	3.9					
ABSG, air-attrited (cal. 1000°C, 3 hr)	0.78	1248	87.1	6.7	2.5	3.8					
ABSG, air-attrited (cal. 900°C, 1 hr)	0.78	1432	86.0	7.6	2.5	3.8	3444	65.6	13.8	7.3	13.3
ABSG, water-attrited	0.86	2165	88.9	4.5	3.0	3.7	5115	62.3	13.3	8.9	15.5
ABSG, water-attrited	0.92	2196	85.5	6.6	3.6	4.4	4371	60.8	14.1	9.2	15.9
ABSG, water-attrited (14.4% H_2O adsorbed)	0.94	1857	87.0	5.4	3.3	4.3					
RA-1 untreated	0.70	417	84.8	10.2	2.3	2.7	942	65.6	17.3	7.5	9.5
Catalyst											
ABSG, air-attrited	1.20	1768	85.3	6.4	3.3	5.0	4036	64.5	13.2	7.4	14.4
ABSG, air-attrited (cal. 900°C, 1 hr)	1.18	1758	87.2	6.0	3.2	3.7	4045	61.6	13.7	8.6	16.1

[a] 0.23-in. depth, 0.5-in.-diam mold.

A hypodermic needle metered N_2H_4 onto the catalyst and the temperature transient (Fig. 3) was plotted by an X-Y recorder. With special bell jar, ambient pressure was varied from vacuum to 760 torr, and the effects of various gases, such as N_2, NH_3, and O_2, were also investigated. The volume of the bell jar reactor (400 cm^3) was large enough so that the pressure fluctuation during the injection of N_2H_4 did not exceed 1 torr.

Previous observation of high-speed color movies of transparent reactor firings had indicated that the activity of the catalyst is affected by the quantity of liquid N_2H_4 loaded onto each granule and that if this ratio was too large, the quenching effect of the excess liquid could cause performance deterioration. The N_2H_4/catalyst saturation ratio, shown in Fig. 4 in terms of mesh size, indicates the amount of N_2H_4 needed to fill the granular pore volume. Initial temperature change ΔT is plotted against the ambient pressure in the bell jar, Fig. 5. No significant difference was observed in ΔT for $\frac{1}{8}$-in. pellets, 25–30 mesh, 14–18 mesh, and 8–12 mesh granules in this pressure range. Pressure less than 30μ produced evaporative cooling to temperatures as low as the freezing temperature of N_2H_4, and in some cases as low as −9°C (super-cooling). Exothermic decomposition of N_2H_4 was then delayed up to 10 sec while the catalyst thawed out. This delay permitted deeper than normal penetration of liquid N_2H_4 into the porous catalyst with consequent severe spalling of the $\frac{1}{8}$-in. pellets. This observation tends to support the postulation that a primary catalyst breakup mechanism is high internal pressure generated by very rapid decomposition of N_2H_4 accumulated in the pores. In the same tests, catalyst granules did not spall, and this is attributed to their more open-pore structure (Fig. 6). The

Table 4 Repeated loads[a]

ABSG carrier used	Wt., g	Cycles	$\bar{P}$, psi	Final deflection, in.	Avg. wt %, U.S. sieve size >30	30–40	40–50	<60
Carrier only								
Air-attrited	0.84	5	2083	0.024	76.7	11.4	5.4	6.5
		20	2175	0.030	69.9	13.5	6.8	9.8
		100	2094	0.038	59.6	15.4	9.0	16.1
Water-attrited	0.85	5	2302	0.024	82.7	6.6	4.6	6.1
		20	2282	0.033	72.9	10.3	6.5	10.3
		100	2450	0.037	61.7	13.1	8.6	16.5
Air-attrited (cal. 900°C, 1 hr)	0.79	5	1355	0.024	81.5	9.9	3.5	5.1
		20	1250	0.027	77.5	11.2	3.9	7.4
		100	1289	0.036	64.8	15.4	7.1	12.8[b]
Catalyst								
Air-attrited	1.20	5	1808	0.024	79.1	9.1	4.4	7.4
		20	1783	0.031	67.6	12.1	6.4	13.9
		100	1768	0.037	63.9	13 0	7.7	15.5
Air-attrited (cal. 900°C, 1 hr)	1.18	5	1763	0.023	81.2	8.5	4.3	6.0
		20	1661	0.027	74.4	10.8	5.7	9.1
		100	1701	0.035	64.7	13.2	7.8	14.4

[a] 0.23-in. depth; 0.50-in. mold; 0.02-in. initial deflection.
[b] Two samples.

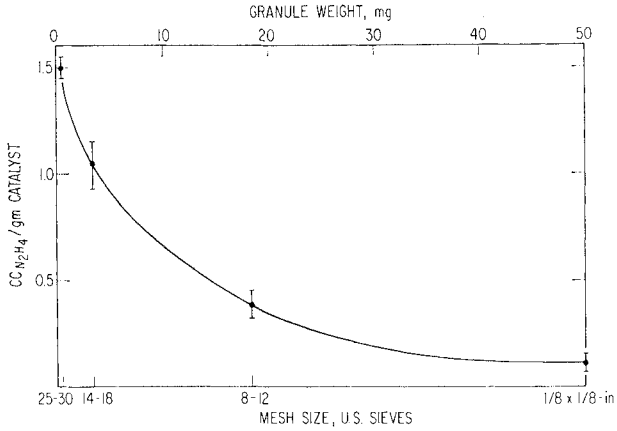

Fig. 4 Saturation loading of hydrazine to catalyst.

evaporative cooling effect diminished with increasing pressure until, at 16 torr, no ΔT was recorded within the first 500 msec of injection. At still higher pressures, the magnitude of ΔT increased, reaching 70°C at 760 torr. In all these tests, ΔT increased at a rate of 420°C/sec, the limiting response of the thermocouple-recorder system.

Measured ΔT is determined by a balance between the exothermic catalytic reaction and the endothermic evaporation of liquid N_2H_4. The catalytic heat release is proportional to the rate and depth of liquid penetration into the porous catalyst. Penetration is controlled by the positive ambient and capillary pressures and the negative back pressure due to accumulating decomposition gases. Since the capillary and back pressures are fixed by the pore structure, the ambient pressure determines the penetration depth, heat release, and temperature rise. At a pressure of 16 torr, the catalytic heat release just equals the evaporative heat loss, so that at higher pressures, the exothermic reaction is dominant. Because no plateau was reached at 760 torr, the initial temperature rise should continue to increase with increasing pressures above atmospheric. This is an important consideration in reactor motor firings where the confined volume leads to a rapid pressure buildup.

The rate and magnitude of the ΔT associated with liquid N_2H_4 at 25°C are much greater than for gaseous N_2H_4 because the liquid penetration rate, from the action of the ambient and capillary forces, is much faster than the rate of gaseous diffusion. However, once the first monolayer of liquid has reacted, an excess of liquid can retard, and even quench, the reactions due to its high heat capacity. Liquid is needed

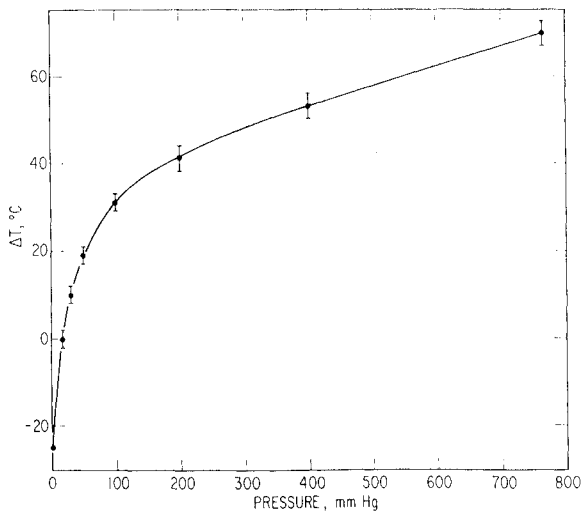

Fig. 5 Temperature rise vs ambient pressure.

Table 5 Thermal expansion test results

Specimen	Initial length, mm	Net change[a] at 1000°C, mm	Net change[a,b] after one cycle, mm	Shrinkage after one cycle, %[b]
AAT ⅛	3.33	−0.040	−0.16	4.81
ABSG 25–30 mesh, air-attrited:				
1st cycle	15.0	+0.015	−0.075	0.50
2nd cycle	14.9	+0.050	−0.110	0.74
3rd cycle	14.8	+0.085	−0.06	0.41

[a] + expansion; − contraction.
[b] cycle: 25°C → 1080°C → 25°C.

for a fast ignition, but the liquid/catalyst ratio must be optimized to ensure the most rapid rate of temperature and pressure rise into the regime of film boiling.

The ΔT at a given pressure was found to be independent of the ambient gas. The same initial increase was observed with O_2 as with N_2. However, a large secondary peak was observed as oxygen diffused into the pores to react with excess liquid N_2H_4. It is apparent that the state of the catalyst in terms of intrinsic activity, surface area, and cleanliness of the iridium (Ir) determine ΔT at a given pressure.

At 25°C, in air, the as-received catalyst[4] has approximately 0.3 atoms of chemisorbed O_2 per atom of Ir. The first ignition, therefore, involves oxidation of N_2H_4 in addition to decomposition. This O_2 layer is removed for subsequent vacuum firings reducing the net heat release. A test was made to measure ΔT with reduced Ir. The catalyst was reduced in H_2 at 400°C and allowed to cool to 25°C under H_2 before N_2H_4 was applied. A ΔT of 27 ± 2°C was observed, compared to 70°C with as-received catalyst.

A ΔT of approximately 3°C, due to heat of wetting, is shown for N_2H_4 applied to granule or pellet of alumina. This contribution is small compared with the catalytic reaction.

The rate and magnitude of ΔT also were studied as a function of the initial catalyst temperature (Table 6). Above 25°C, the rise was limited by a peak temperature of 95 ± 5°C; at lower temperatures, the magnitude and rate of ΔT decreased. An Arrhenius activation energy was calculated from the temperature dependence of the rate of rise. The value, 3 kcal/mole, is actually a pseudo activation energy, since 25°C N_2H_4 was applied to cooler catalyst. This experiment simulates motor firings where N_2H_4 at storage temperature is injected into a precooled reactor. The temperature dependence of low-temperature ignition delay data[5] indicates a comparable activation energy.

Surface Area

Adsorbed O_2, the surface area of the Ir and the porosity of the carrier mainly determine catalyst activity. The factors that determine the active surface area are: the area of the alumina substrate, metal loading, and the thermal history of the catalyst during processing and use. Each of these factors is demonstrated in Table 7. First, precalcining of the ABSG carrier at 900°C decreases the alumina surface area (as measured by N_2 gas adsorption) approximately 50% relative to uncalcined carrier.[6] When 31 to 33 wt. % Ir is deposited on this calcined carrier, the resulting metal area, as measured by H_2 chemisorption, is less than 50% of the typical catalyst value.[6] The H_2 adsorption corresponds to approximately one H atom per exposed metal atom; thus,

Table 6 Initial temperature rise

T_i, °C	T_f, °C	dT/dt, °C/sec
−20	20	220 ± 30
0	57	280 ± 30
25, 40, 50, 60, 75	95	420 ± 40

Table 7 Surface areas

Catalyst	Area, m^2/g	H_2 sorption,[a] μmoles/g
Typical 405	110–130	340–400
ABSG (precalcined carrier, 900°C)	55–70	110–160
Annealed ABG (H_2, 1 hr, 1800°F)	~60	~180 (est.)
Annealed ABG (A, 1 hr, 1800°F)	~47	<100 (est.)
Motor-fired ABG (1 hr, 1800°F)	~75–80	~200 (est.)
AAT $\frac{1}{8}$ (24.6 wt % Ir)	110–130	~330
ATT $\frac{1}{8}$ (8.7 wt % Ir)	110–130	~200
ABSG (22.5 wt % Ir)	110–130	~300
ABSG (18.7 wt % Ir)	110–130	~280

[a] Approximately ten times metal surface area in m^2/g; (est.) = estimated.

a H_2 chemisorption of 350μ moles/g of catalyst means a metal surface area of about 35 m^2/g.

On a weight basis, the addition of Ir reduces the total surface area, measured by N_2 adsorption, by the wt% of Ir making up the catalyst. Thus, catalyst made from 160 m^2/g alumina will have a total surface area of approximately 110 m^2/g.

The catalyst total and metal surface areas are both decreased after thermal conditioning at 1800°F. A greater loss occurred in a neutral (argon A) atmosphere than in a reducing (H_2) atmosphere.[3] Surface diffusion and sintering of Ir, promoted by the presence of initially chemisorbed O_2, apparently occurs more readily in a neutral atmosphere.[4,7] Electron micrographs were taken of the surface of Shell 405 pellets which had been heated in H_2 and in A for 1 hr at 1000°C. The micrographs indicate more metal sintering in the A atmosphere. Metal crystallites appeared to diffuse and concentrate in ridges during the heat treatment; also, larger alumina crystallites were formed through partial recrystallization of the substrate.

Motor-fired catalyst (reducing atmosphere) seems to suffer a lower loss of surface area than H_2-annealed catalyst. This is probably because the entire bed did not reach the peak operating temperature of 1800°F during steady-state firing conditions.

The active metal surface area does not increase linearly with catalyst metal content. Several pellet and granule samples with reduced metal loadings were supplied by Shell Development Company for activity testing. The activities of two pellet and granule catalysts included in Table 8 were identical to the activity of the standard 405 catalyst. Only the pellet sample (8.7 wt %Ir) indicated a decrease in activity (~70%) after annealing in H_2 for 1 hr at 1800°F.

Hydrogen annealing probably reduces the active metal area of the 405 catalyst by at least 50%. The pellet sample with 8.7 wt %Ir, therefore, is estimated to have a H_2 sorption value of about 100 after H_2 annealing. ABSG prepared with precalcined carrier retains the same thermocouple activity as standard 405, although the H_2 sorption values greater than 100 remain undifferentiated by the laboratory test. Activity can be discriminated through ignition delay time to H_2 sorption values lower than approximately 200, i.e., there is a significant increase in the ignition delay time compared to standard 405 catalyst. The laboratory thermocouple test at atmospheric pressure, therefore, is not as sensitive in indicating activity as ignition delay in an actual motor test.

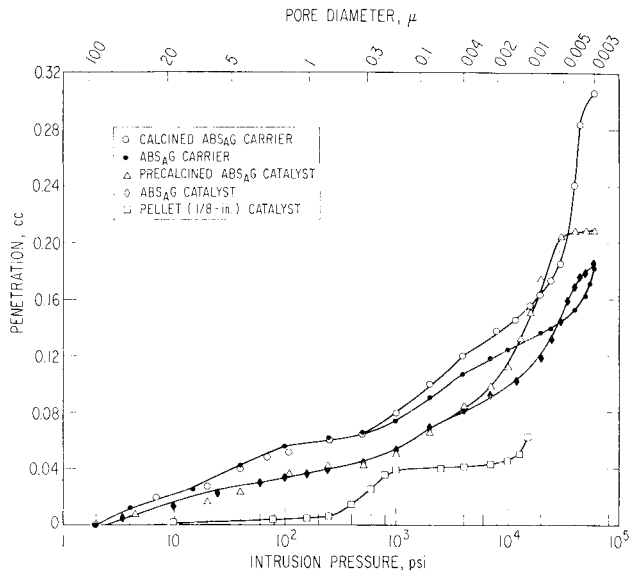

Fig. 6 Catalyst porosity.

Porosity

Mercury intrusion porosity determinations were made of three catalysts and two carriers. A plot of the data, normalized to 1 g, is given in Fig. 6. Calcining (900°C, 1 hr) 25–30 mesh ABSG air-attrited carrier opened the smaller pores (<0.3μ) relative to uncalcined carrier, thus increasing the pore volume approximately 70%. However, the surface area was reduced about 50% in the process (Table 7). The smaller pores were opened through the loss of interstitial and combined water. The corresponding catalysts (air-attrited and precalcined ABSG) display decreased porosity due to the Ir loading of the carrier. Again, the two catalysts showed a distinct difference in pore size below 0.05μ. The pore distribution curve for the $\frac{1}{8}$-in. pellet catalyst indicates tighter-packed, less-open structure than for the granular catalyst. Since the carrier used in the pellet was obtained from a different company than the carrier used in the granules, and since the manufacturing process involved pelletizing rather than simple air drying of the alumina gel, such pore size differences were reasonable.

Motor Firings

The experimental apparatus was similar to that used in previous monopropellant N_2H_4 testing.[5] The test unit consists of: a stainless steel N_2H_4 reservoir pressurized to 300 psi by N_2 gas; a propellant solenoid valve; a stainless steel (thermal-standoff) injector with a 0.024-in. diam (single) orifice; a 40 × 50 mesh inconel injection screen; a 0.5-in. diam bed of 25–30 mesh catalyst 0.58-in. long; a 60-mesh stainless steel catalyst support screen welded to a support-spacer; and a 50 to 1 expansion ratio nozzle with a 0.088-in.-diam throat. The design characteristics of this reactor are listed in Table 2.

The reactor chamber pressure was measured by a strain-gage transducer mounted on a 3-in.-long thermal standoff tube located between the bottom of the catalyst bed and the nozzle. The output of the transducer was conditioned and

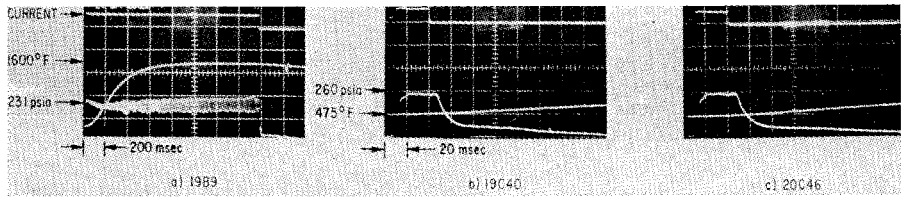

Fig. 7 Typical motor firing performance.

Table 8 Comparison of motor firings

Type of catalyst	Duty[a] cycle	$\bar{T}_c$, °F	$\bar{T}_{cm}$, °F	$\bar{P}_c$, psia	Catalyst loss, %	Standard deviation σ, %
ABSG, air-attrited, precalcined	A	289	...	224		
	B	314	1625	232	3.60	0.46
	C	447	...	254		
ABSG, standard	A	307	...	230		
	B	336	1624	223	5.56	0.25
	C	465	...	245		
ABSG, air-attrited	A	310	...	223		
	B	317	1603	229	5.67	0.33
	C	481	...	250		
ABG	A	302	...	247		
	B	312	1635	245	5.06	0.47
	C	475	...	264		

[a] A) Fifty 40-msec pulses 60 sec apart; B) ten 1.6 sec pulses 5 min apart; and C) same as A.

Table 9 Motor-firing[a] results, breakup and loss

Process	Average wt %, U.S. sieve size 30	30–40	40–60	60	Loss
Catalyst					
a) Before firing					
ABSG, air-attrited	99.3	0.7	<0.1	<0.1	...
ABSG, air-attrited (calcined carrier)	99.3	0.7	<0.1	<0.1	...
b) After firing					
ABSG, water-attrited	92.8	3.5	2.0	1.7	5.6
ABSG, air-attrited	93.5	3.8	1.5	1.2	5.7
ABG	95.0	3.0	1.1	0.7	5.1
ABSG, precalcined, air-attrited	95.2	2.9	1.2	0.8	3.6

[a] See Tables 2, 8 and Fig. 7.

amplified for display on an oscilloscope and on a visicorder. Reactor discharge temperature was instrumented using an alumel-chromel thermocouple located on the motor centerline between the support screen and the catalyst. An amplifier was used to raise the output signal to a level suitable for recording on the visicorder and a differential amplifier was used for monitoring on the oscilloscope. The circuitry used to actuate the solenoid valve consisted of a dual-cycle and was also used to actuate the visicorder 100 msec before actuating the valve (to save paper). The amplifier converted the counter output to a level suitable for valve actuation. The valve coil current was also monitored and recorded, by using a 0.26 ohm sampling resistor in series with the valve coil, to provide a measure of the valve open time. All of the data were obtained from the visicorder traces, with occasional sample polaroid photographs of the oscilloscope display, Fig. 7.

The motor firings were performed at an average vacuum pressure of 800–1000μ with a standard duty cycle consisting of fifty 40-msec pulses 60 sec apart (A), ten 1.6 sec pulses 5 min apart (B), and fifty 40-msec pulses 60 sec apart (C). The catalyst was weighed before and after the tests to determine the amount of catalyst lost through 60-mesh support screen and the remaining catalyst was sieved to determine the degree of breakup. Three series of firings were performed with each of the following types of catalyst: the early ABG catalyst; the newer ABSG catalyst, both air and water-attrited; and precalcined catalyst.

The results are summarized in Tables 8 and 9. A comparison of average initial catalyst temperature $\bar{T}_c$, average steady-state catalyst temperature $\bar{T}_{cm}$, and average chamber pressure $\bar{P}_c$, indicates that there is very little difference in performance between each of the four types of catalyst tested (see also Fig. 7). There is also no significant difference in the amount of catalyst loss and breakup between the ABG catalyst and the newer ABSG catalysts, air or water-attrited. Only the precalcined catalyst is $\frac{1}{3}$ lower in catalyst loss and breakup.

Possible reasons for improved durability of the calcined catalyst were explored. The crush test results, Tables 4 and 5, do not show that the precalcined catalyst has superior strength. However, the gas blast tests at 10% void space, Table 1, show that the precalcined catalyst has less loss than the noncalcined catalyst. Although none of the catalysts was damaged in the thermal shock tests, thermal expansion data, Table 5, indicates that the catalyst shrinks after firing. Such shrinkage tends to create a void space in the catalyst bed and the gas blast results show that the amount of catalyst loss is a function of void space (as mentioned, the precalcinating process originated in an attempt to alleviate catalyst shrinkage).

In addition, during the laboratory catalyst activity tests, it is observed that catalyst spalling or breakup is apparently a function of the catalyst pore size distribution. The porosity measurements, Fig. 6, show that the precalcined catalyst has a more open pore structure relative to the uncalcined catalyst. If a postulated[5] primary mechanism of catalyst breakup due to high internal pressure in the catalyst granules generated by rapid decomposition of accumulated N_2H_4 is accepted, then a catalyst with an open pore structure would be more durable.

Conclusions

For the conditions tested, there were no measurable differences between the catalysts in activity or in motor performance. Also, no significant differences in postfiring catalyst breakup and loss were observed between the early ABG catalyst and the newer ABSG catalysts, either air or water-attrited. Although not clearly superior in mechanical crush strength, $\frac{1}{3}$-reduction in loss is obtained with precalcined catalyst. Laboratory tests indicate that reasons for this improvement in durability are probably a) the development of less free space in the catalyst bed, due to a lower amount of catalyst shrinkage, and b) a reduction in internal shattering of the catalyst granules, due to a more open pore structure which alleviates high-intragranular pressure.

References

[1] Newsome, J. W. et al., "Alumina Properties," Technical Paper 10, 1960, Alcoa Research Lab., Pittsburgh, Pa.

[2] Price, T. W. and Evans, D. D., "The Status of Monopropellant Technology," T. R. 32-1227, Feb. 1968, Jet Propulsion Lab., Pasadena, Calif.

[3] Carlson, R. A. and Baker, W., "Space Environment Operation of Experimental Hydrazine Reactors," Rept. 4712-4-67-28, April 1967, Thompson Ramo Wooldridge Corp., Redondo Beach, Calif.

[4] Carlson, R. A., Blumenthal, J. L., and Grassi, R. J., "Space Environmental Operations of Experimental Hydrazine Reactors," Rept. 4715.3-68-27, July 1968, Thompson Ramo Wooldridge Corp., Redondo Beach, Calif.

[5] Greer, H., "Vacuum Startup of Reactors for Catalytic Decomposition of Hydrazine," *Journal of Spacecraft and Rockets*, Vol. 7, No. 5, May 1970, pp. 522–529.

[6] Williams, P., private communication, July 1968, Shell Development Co., Emeryville, Calif.

[7] Schafer, H., *Chemical Transport Reactions*, Academic Press, New York, 1964, p. 38.